0273-2289/89/2021—0449$02.40

Dispersion and Holdup in a Three-Phase Fluidized-Bed Bioreactor

BRIAN H. DAVISON

Chemical Technology Division, Oak Ridge National Laboratory, Oak Ridge, TN 37831-6226

ABSTRACT

Axial dispersion and phase holdup measurements were made using electroconductivity in a fermenting fluidized-bed bioreactor (FBR) and in a model nonfermenting three-phase FBR. Multiple axial conductivity probes were used to nonintrusively monitor the bed conductivity. The gas phase holdup was estimated from a ratio of the average bed conductivity and bulk conductivity. The solid fraction in the three-phase FBR can be estimated from the two-phase liquid–solid FBR. The response to a salt pulse was used to estimate the liquid axial dispersion coefficient. Particle Peclet numbers on the order of 10^{-2} were estimated as a function of flowrates and compared to literature correlations.

Index Entries: Three-phase; fluidized-bed bioreactor; columnar hydrodynamics; fermentation.

INTRODUCTION

Columnar bioreactors using immobilized biocatalysts have gained interest because of their potential advantages of higher volumetric productivities and greater conversion. In alcohol production, for example, the highest productivity reactors are all columnar reactors (*1*). Many columnar bioreactors have three phases: the liquid media, the solid biocatalyst, and a gas phase, which is either produced (such as CO_2) or provided as a nutrient (such as oxygen). Three-phase columnar fluidized-bed reactors (FBR) present a special challenge to the biochemical engineer because the hydrodynamics of three-phase FBRs are poorly characterized even in traditional catalytic chemical systems; and simple models, such as ideal plug-flow, are often inadequate to evaluate and scale these systems.

(Muroyama and Fan (2) have written an excellent review of the current status of the hydrodynamics of three-phase fluidization.) In addition, the existing correlations and techniques were not developed in the ranges of flow or particle size and density that are of interest in a bioreactor. Techniques and correlations need to be developed and confirmed in three-phase columnar bioreactors for the estimation of important hydrodynamic parameters such as phase holdup, dispersion, and interphase mass transfer.

Fermentation in a FBR presents an additional challenge in that the gas flow varies with axial position. Carbon dioxide is a coproduct with ethanol from sugar. Thus, the conditions in the reactor change from just liquid and solid at the inlet, to a three-phase system as increasing amounts of gas are produced.

Background

Traditionally, phase holdup in a fluidized bed has been estimated by the following equations.

$$\epsilon_L + \epsilon_G + \epsilon_S = 1 \tag{1}$$

$$dP/dh = g(\epsilon_L \cdot \rho_L + \epsilon_G \cdot \rho_G + \epsilon_S \cdot \rho_s) \tag{2}$$

$$\epsilon_S = V_s / V_{bed} \tag{3}$$

The first equation is the sum of the phase fractions, ϵ_G, ϵ_L, ϵ_S, for the gas, liquid, and solid, respectively. The second equation relates the pressure drop to the average bed density, while neglecting the frictional effects. The third calculates the average solid fraction across the bed as the ratio of the volume of the solid added, V_s, over the volume of the bed, V_{bed}. This assumes that the solid fraction is uniform throughout the bed, which is generally true for constant flowrate FBRs but may not be applicable to gas generating systems.

Unfortunately, it is difficult to use the pressure drop in a laboratory-scale three-phase FBR because the pressure drops are small (< 4 cm H_2O) and the density of the solid approximately equals that of the liquid. Electroconductivity was proposed and successfuly tested as an alternative by Begovich and Watson (3) in a nonreactive system of air, glass beads, and aqueous electrolyte. In their system, the glass and the gas were nonconductive. This allowed the liquid fraction to be measured as the ratio of the overall measured bed conductivity, γ, to the liquid electrolyte conductivity, γ_o. In the present system, the solid gel beads are very permeable and have the same conductivity as the surrounding electrolyte. Therefore, only the gas is nonconductive. Conductivity measurements of mixtures of gel beads and electrolytes showed that the conductivity of the gel was within 2% of the conductivity of the surrounding electrolyte. Therefore, Eq. (2) can be replaced by

$$\gamma/\gamma_o = \epsilon_L + \epsilon_S = 1 - \epsilon_G \quad (4)$$

and used to nonintrusively measure the gas fraction along the column.

An additional advantage of using conductivity measurements is that conductivity has long been used in dispersion experiments to monitor the response of a system to an impulse or step-change of salt tracer. The axial dispersion of a solute in a nonreactive system can be modeled as

$$dC/dt + u_L\, dC/dz = D\, d^2C/dz^2 \quad (5)$$

where C is the concentration, D is the liquid axial dispersion coefficient, and u_L is the liquid velocity. After nondimensionalization, the Peclet number, which is a ratio of convective to dispersive forces, is defined as

$$Pe = u_L d_p / D \quad (6)$$

where d_p is the particle diameter. Then the method of moments can be used according to Stiegel and Shah (*4*) to calculate the residence times and the Peclet numbers from the response to an arbitrary tracer impulse that moves between two probes.

MATERIALS AND METHODS

The bead production technique has been described previously (*5*). The preliminary conductivity measurements of various solutions were performed with a radiometer conductivity meter and probe (cell constant = 1 cm) in a well mixed, constant-temperature bath.

Gel beads were made with and without cells and iron oxide. They were then equilibrated with 0.1 *M* KCl at 30°C. The conductivity was measured in a liquid-solid system at various flowrates in order to change the solid fraction from zero to that of a packed bed. The conductivity change decreased by less than 2% in the presence of the solid gel with or without the added iron oxide. Therefore, the conductivities of the gel and the electrolyte was taken to be identical and the gas fraction estimated by Eq. (4).

The columnar reactor used for the conductivity experiments was water jacketed at 30°C, 2.54 cm ID, and 650 mL in volume. Sample ports and the conductivity probes were placed at ~30 cm intervals along the column as shown in Fig. 1. The conductivity probes were platinum foil squares (1.27 cm) mounted on opposite sides of the 2.54 cm ID column. They were connected to three Radiometer conductivity meters with output to a multiple chart recorder. The probes were individually calibrated. The multiple electroconductivity probes were also interfaced with an IBM-PC through an ISAAC-2000 computerized data acquisition system. The raw data were sorted every 3 s on disc at a rate of 1 sample per probe.

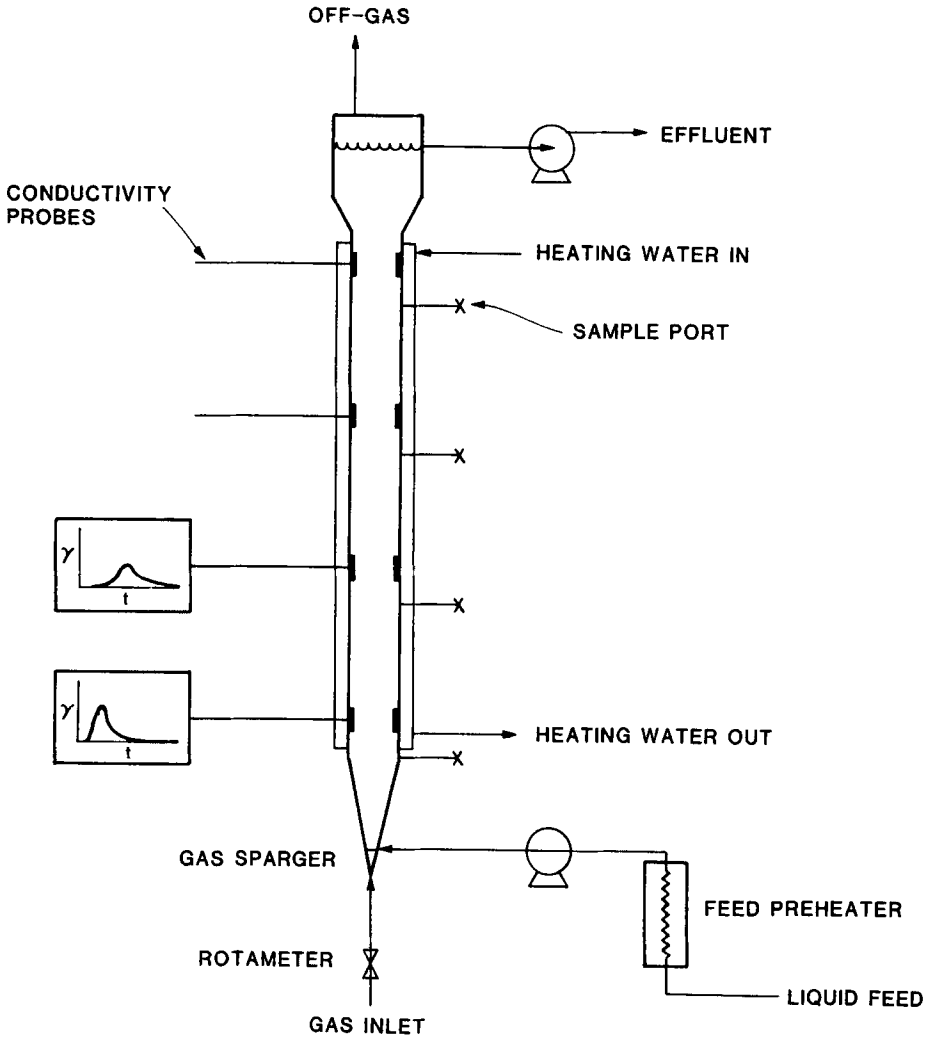

Fig. 1. Schematic of fluidized-bed reactor for holdup and dispersion measurements by electroconductivity.

In the inert (inactive-bed experiments) the column was filled with 0.12-cm-diam gel beads. The sparge gas (air) was metered through a ball rotameter and introduced to the bottom of the column through a medium glass frit. The liquid was introduced through radial inlets directly above the gas sparger. This method provided small bubbles and uniform flow similar to that at the bottom of a fermenting FBR. At constant gas and liquid flowrates, ranging from 0 to 20 and 0 to 5 L/h, respectively, data were collected for 10 min to establish the average holdup and a baseline for the dispersion measurements and for the calculation of average gas holdup. Then a 10 mL pulse of 3 *M* KCl was injected into the liquid flow inlet; the tracer response data were continued to be collected as the pulse traveled up the column.

Figure 2 illustrates the raw data from a typical run. The chart response (in arbitrary conductivity units) of the three probes has been offset vertically for visual clarity. The increase in "noise" of the response from the bottom of the column to the top is a result of bubble coalescence, which causes larger fluctuations in the conductivity as the bubbles pass the probe. Before the injection, the baseline conductivity data were directly averaged and divided by the bulk conductivity to give the average gas holdup. The raw conductivity data were smoothed, and the first and second moments of the response curves were calculated by integration using Simpson's Rule. The dispersion coefficient can be estimated from the difference of these moments.

The reactor was operated at various flowrates of gas and liquid (0.5 *M* KCl) for at least 1 h to establish stable conditions. The bed or bed volume, V_{bed}, was estimated visually to within 25 mL, neglecting the small amount of entrained beads above the bed.

Fermentations using immobilized *Z. mobilis* in a FBR and the procedures for culturing, immobilization, and analysis have been described previously (*6*). In the holdup experiments in an active fluidized-bed bioreactor with immobilized *Z. mobilis* NRRL 14023, the feed medium used was 10% glucose, 0.5% yeast extract, and 0.05 *M* KCl. Similar holdup and pulse response experiments were performed at two steady-state flowrates with beads of 0.084 cm diam.

RESULTS AND DISCUSSION

Glucose and ethanol were shown to have a negative linear effect on the conductivity of a 0.1 *M* KCl solution at 30°C. The conductivity falls from the base value of 13.9 mS to 83% and 74% of the base value for glucose and ethanol, respectively, at a 10% concentration. This effect is additive, and the conductivity of mixtures of ethanol and glucose in electrolyte can be accurately predicted. Yeast extract and cells were separately observed to have a positive linear effect on the electrolyte conductivity but the effect was always less than 5% for the ranges of interest (0–10 g/L yeast extract and 1–20 g dry wt/L cells).

Phase Holdup

Twenty runs were performed with the inactive FBR and data collected at a variety of flowrates ranging from 0 to 5 and 0 to 23 L/h for the gas and liquid, respectively. Figure 3 shows the effect of liquid flow on solid holdup in the two-phase system (no gas). As expected, the solids fraction smoothly decreases with increasing flow rate. Figure 4 shows the effect of increasing gas flow on the solids fraction at two liquid flowrates. The solids fraction is a weak function of gas flowrate. This data illustrates the good gas disengagement properties of the FBR.

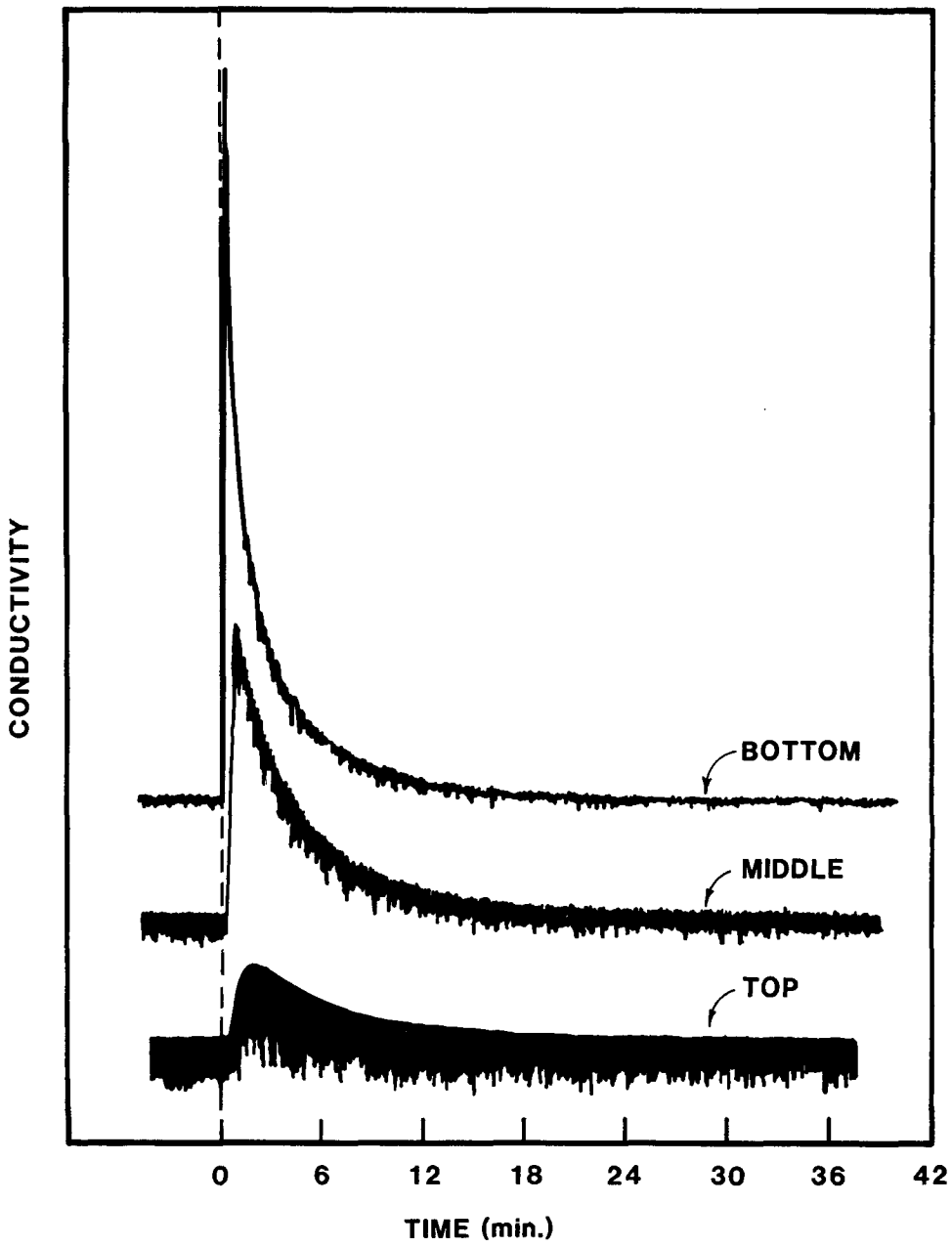

Fig. 2. Raw conductivity response data for a holdup-dispersion run at $F_L = 5$ L/h and $F_G = 23$ L/h. Ten mL of 3 *M* KCl injected at time zero.

A further observation of the data from the 3 L/h liquid flow is an apparent bed contraction with low gas flowrates in a liquid fluidized-bed. This contraction effect was also observed previously in a three-phase FBR with dense fine particles (*7–9*) and with 1 cm plastic beads (*10*). It was also reported that a further increase of either the gas or electrolyte flow rate will negate this effect (*10*), as is observed from the data in Fig. 4. These

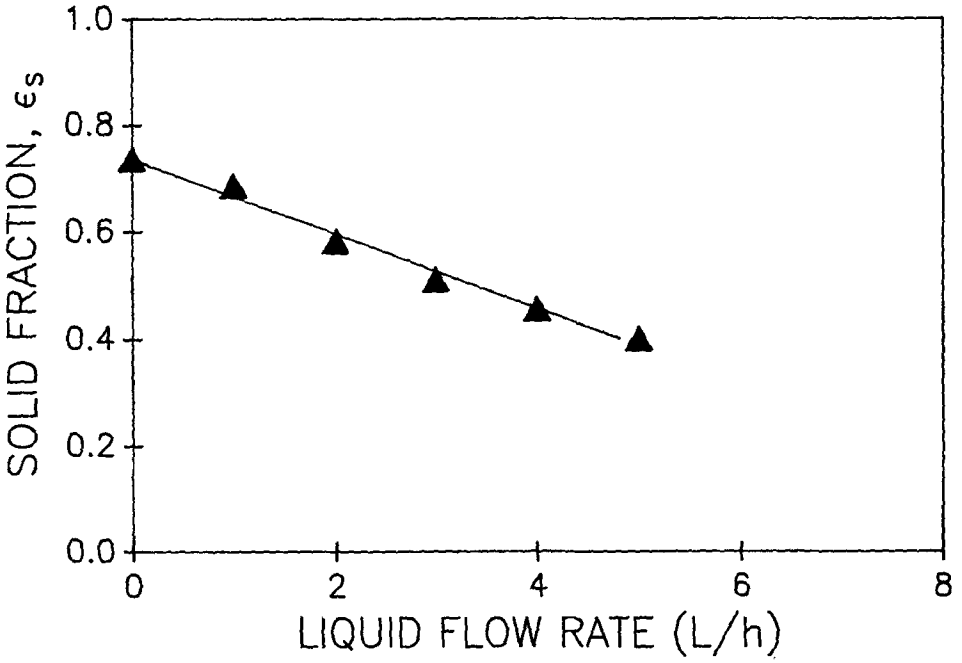

Fig. 3. Solid holdup in a two-phase FBR with no gas flow. (2.54 cm-ID column).

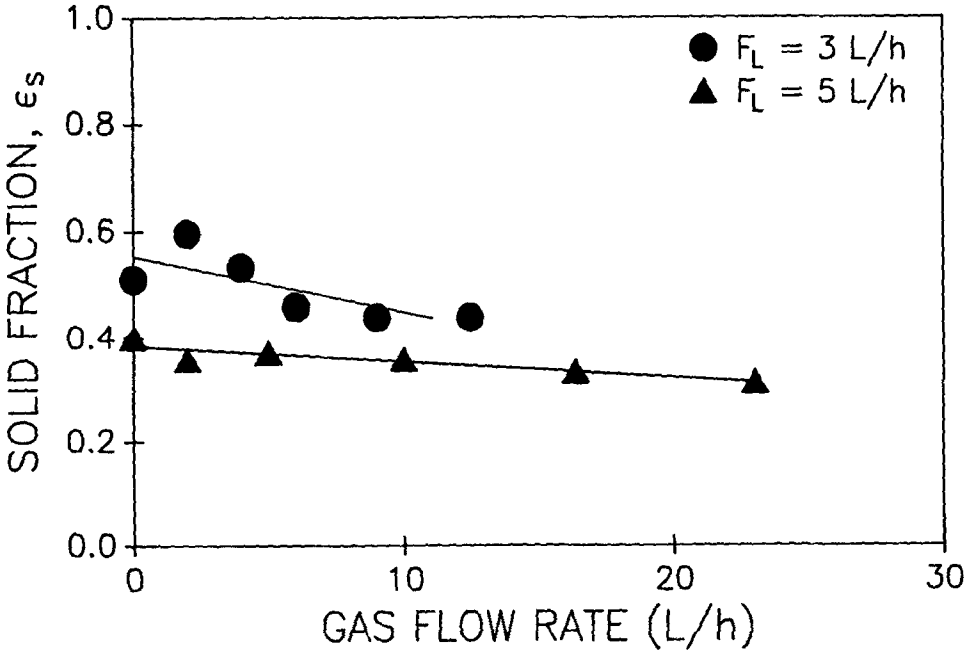

Fig. 4. Solid holdup in a three-phase FBR as a function of gas flow.

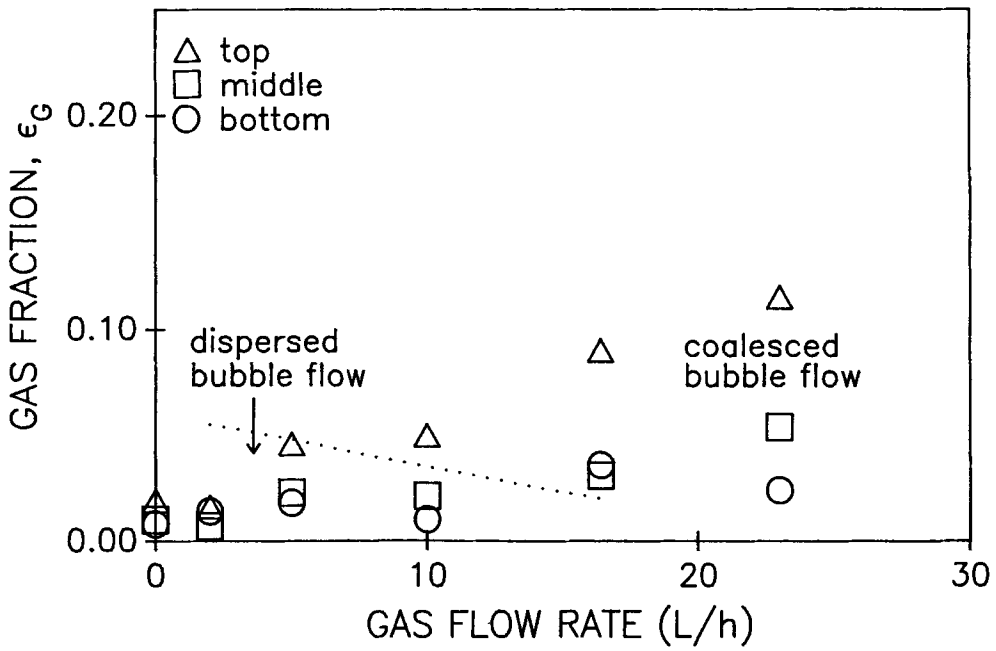

Fig. 5. Gas holdup in a three-phase FBR.

observations indicate that there are hydrodynamic differences between fluidized-beds with low density solids and those with the dense glass and metal particles typically used to develop hydrodynamic correlations (which do not show this effect). Kim et al. (9) reported a critical particle size and density, which governs the transition from a bubble coalescing and a bubble disintegrating regime.

The conductivity data collected over a 10-min interval at constant conditions were averaged and the gas fraction calculated using Eq. (4). Small bubbles were released from the frit but coalesced as they rose up the column, and the presence of bubbles caused fluctuations in the conductivity as they passed the probe. The magnitude of these fluctuations increased as the bubbles coalesced, requiring the use of an average conductivity. The average gas fraction appeared to be controlled by the bubble size.

Figure 5 shows the gas fraction as a function of gas flowrate at constant liquid flow. Qualitative visual observation indicated two bubble flow regimes in the FBR: a dispersed bubble regime and a coalesced bubble regime. The dotted line roughly separates these two bubble-flow regimes. The gas fraction is neglibible in the dispersed-bubble regime, which occurs at low gas rates and near the bottom of the column. In the coalesced-bubble regime, where the bubbles' diameters approach the column diameter, the gas holdup cannot be predicted without further study of coalescence in this system. Direct measurement of the gas fraction in fermenting FBRs by online conductivity probes may allow better modeling and operation control.

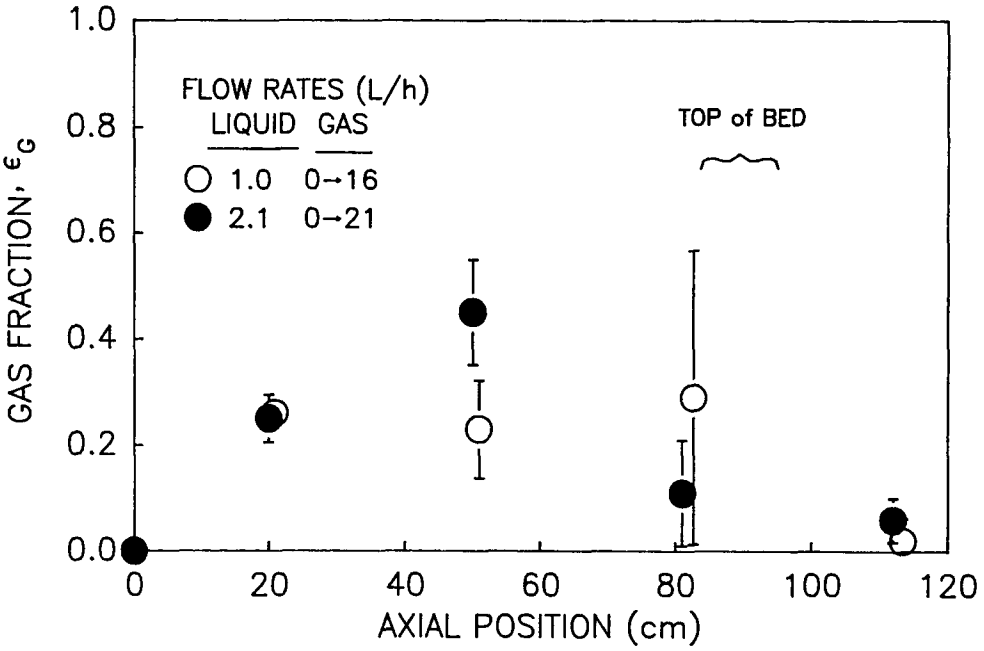

Fig. 6. Axial gas holdup in a fluidized fermentor: 250 mL of immobilized *Z. mobilis* in 0.084 cm diam beads fed with 10% glucose and 0.05 *M* KCl.

The fermenting FBR was filled with 250 mL of gel beads containing 4% κ-carrageenan, 3% iron oxide, and an initial concentration of about 15 g dry wt/L cells of *Z. mobilis*. The FBR was fluidized with a liquid flow rate of 1 L/h and operated for 3 d to reach stable conditions. After sampling and making the conductivity and dispersion measurements, the flowrate was increased to 2.1 L/h. The next day the measurements were repeated at this latter condition. Liquid samples were taken and their conductivity measured externally in order to compensate for effects from the changing solute concentrations.

Conductivity readings from each axial probe were collected for 30 min, averaged, and the standard deviation calculated, as shown in Fig. 6. The conductivity measurements had increasingly larger fluctuations in response to passing bubbles, as described above. The gas fraction may increase along the column as gas is produced and bubble coalescence occurs. Near the top of the bed the gas fraction drops, as the gas freely escapes in the essentially two-phase liquid-gas system. These measurements agree with visual observation of the bed.

Axial Dispersion

Dispersion experiments were performed in both the inert and fermenting FBRs, as described above. The first and second moments were calculated by the method of moments, followed by the calculation of the

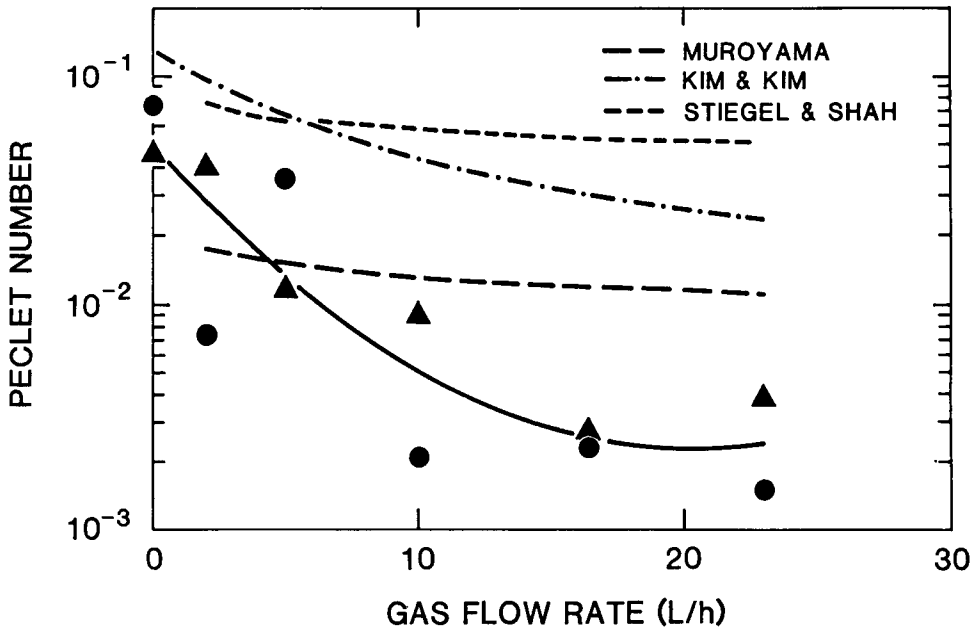

Fig. 7. Experimental Peclet numbers as a function of gas flowrate with $F_L = 5$ L/h. Peclet numbers compared to literature correlations from Muroyama et al. (*11*), Kim and Kim (*12*), and Stiegel and Shah (*4*).

residence times and the particle Peclet numbers. Figure 7 shows the effect of gas flowrate on the Peclet number at a constant liquid flowrate. The experimental data are compared with three semi-empirical literature correlations (*4,11,12*). As expected, the dispersion increases with increasing gas flow. Although the differences among the correlations are comparable to the difference with the experimental data, the experimental values still appear to be lower than the correlations. This effect may be related to the fact that these correlations were developed in systems with high density differences and Reynolds numbers from 10 to 500 or more, whereas, the gel biocatalysts typically have a density of 1.05–1.15 g/L and Reynolds numbers near 1. Calculations (from data not presented here) of experimental Peclet numbers at other flowrates and from the fermenting FBR are comparable to those reported here. Further work is planned to confirm these experimental measurements and to determine an applicable correlation for these biological systems. The form of published correlations may not be applicable, since both the Muroyama (*11*) and Stiegel and Shah (*4*) correlations are undefined at zero gas flow.

CONCLUSIONS

Axial conductivity probes have been demonstrated to be a method for the nonintrusive continuous measurement of the gas fraction within an actively fermenting FBR. The incorporation of numerical estimates of the

gas holdup into the total columnar reactor model have considerably improved the accuracy in packed-bed models (*13*). It is expected that experimental measurements will allow similar improvements in a FBR model.

The solids fraction is a weak function of the gas flowrate and can be reasonably estimated from the two-phase system. Conductivity can also be used to nonintrusively estimate the mixing or dispersion within an active three-phase FBR. This is important because it is difficult to construct a model of an inert FBR with similar three-phase hydrodynamics and gas generation. The conductivity measurements were relatively easy to make; the difficulty lies in smoothing the fluctuations caused by the gas bubbles. The Peclet numbers were found to be in moderate agreement with the correlations of Muroyama (*11*), Stiegel and Shah (*4*), and Kim and Kim (*12*). Further work is planned on the correlation of the gas fraction and dispersion results, and on extending these methods to larger diameter columns to observe possible effects of scale. These measurements will then be incorporated into an overall, three-phase, fermenting FBR model.

ACKNOWLEDGMENT

Research sponsored by the Energy Conversion and Utilization Technologies Program, US Department of Energy, under Contract No. DE-AC05-840R21400 with Martin Marietta Energy Systems, Inc. The Oak Ridge National Laboratory is operated by Martin Marietta Energy Systems, Inc., for the US Department of Energy under Contract No. DE-AC05-840R21400.

The submitted manuscript has been authored by a contractor of the US Government under contract No. DE-AC05-840R21400. Accordingly, the US Government retains a nonexclusive, royalty-free license to publish or reproduce the published form of this contribution, or allow others to do so, for US Government purposes.

REFERENCES

1. Godia, F., Casas, C., and Sola, C. (1987), *Process Biocehm.* **22**(2), 43–48.
2. Muroyama, K. and Fan, L.-S. (1985), *AIChE J.* **31,** 1–34.
3. Begovich, J. M. and Watson, J. S. (1978), *AIChE J.* **24,** 351–354.
4. Stiegel, G. J. and Shah, Y. T. (1977), *Ind. Eng. Chem. Proc. Des. Dev.* **16,** 37–43.
5. Scott, C. D. (1987), *Ann. NY Acad. Sci.* **501,** 487–493.
6. Davison, B. H. and Scott, C. D. (1988), *Appl. Biochem. Biotech. Symp.* **18,** 19–34.
7. Massimilla, L., Solimand, A., and Signorine, P. (1959), *La Ricerca Scientifica* **29,** 1934.
8. Stewart, P. S. B. and Davidson, J. F. (1964), *Chem. Eng. Sci.* **19,** 33.
9. Kim, S. D., Baker, C. G. J., and Bergougnou, M. A. (1972), *Can. J. Chem. Eng.* **50,** 695.

10. Elenkov, D., Nikov, I., and Vlaev, S. D. (1986), *Hungarian J. Ind. Chem.* **14,** 433–441.
11. Muroyama, K. et al. (1978), *Kagaka Kogaku Ronbunshu* **4**(u), 662.
12. Kim, S. D. and Kim, C. H. (1983), *J. Chem. Eng. Japan* **16,** 172.
13. Hamaci, H. and Ryu, D. Y. (1987), *Biotech. Bioeng.* **29,** 994–1002.